

## Peraluminous granites in NE Palmer Land, Antarctic Peninsula: early Mesozoic crustal melting in a magmatic arc

H. E. WEVER, B. C. STOREY & P. LEAT

British Antarctic Survey, Natural Environment Research Council, High Cross, Madingley Road, Cambridge, CB3 0ET, UK

**Abstract:** A suite of Early Jurassic metaluminous to strongly peraluminous granitoids occupy a rear-arc position in Palmer Land, Antarctic Peninsula with respect to a Mesozoic–Cenozoic magmatic arc. Fractional crystallization of a range of mafic to silicic magmas yielded feldspar megacrystic granites, orthogneisses and foliated granodiorites. Leucogranites are strongly peraluminous and have the highest  $^{87}\text{Sr}/^{86}\text{Sr}$  initial ratios of 0.7205–0.7208, somewhat lower than those of older paragneiss. Isotopic and elemental data are used to model generation of leucogranite magma by partial melting of paragneiss, followed by mixing of basalt magma with the crustal melt to form parent magmas of the rest of the granitoids. The crustal partial melting was a result of heat convected by the mafic magma, intruded into an extensional back-arc basin setting contemporaneous with the initial stages of Gondwana break-up. The mafic magma had relatively low  $^{143}\text{Nd}/^{144}\text{Nd}$  ratios, distinct isotopically from the MORB-like basalt thought to represent the mantle input to granitoid genesis in the north western part of the Antarctic Peninsula. The nature of the mantle source(s) of the enriched basalt is uncertain, but it is isotopically similar to approximately contemporaneous basalts associated with the Karoo mantle plume.

**Keywords:** S-type granites, back-arc basins, subduction, Antarctica.

It has been known for many years that the Antarctic Peninsula is a Mesozoic–Tertiary magmatic arc related to east-directed subduction of Pacific Ocean crust (Suárez 1976; Saunders *et al.* 1980; Pankhurst 1982, 1990; Pankhurst *et al.* 1988). The magmatic arc has both volcanic and plutonic rocks, which crop out in subequal amounts. Most of the plutonic rocks form a dominantly metaluminous, calc-alkaline, amphibole-bearing gabbro–diorite–granodiorite–granite association, typical of ensialic magmatic arcs (e.g. Saunders *et al.* 1982; Pankhurst 1990; Harrison & Piercy 1990). Geochemical and isotopic relationships in this association have been regarded as mainly resulting from differences in the importance of high  $^{87}\text{Sr}/^{86}\text{Sr}$  crust versus low  $^{87}\text{Sr}/^{86}\text{Sr}$  mantle-derived magma as sources for its component plutons (Pankhurst *et al.* 1988; Hole *et al.* 1991). This paper describes a different plutonic association within the Jurassic rear-arc in NE Palmer Land, Antarctic Peninsula (Fig. 1). The association is characterized by the presence of distinctly peraluminous compositions, and high initial  $^{87}\text{Sr}/^{86}\text{Sr}$  ratios. We relate the origin of these rocks to the involvement of partial melts of paragneiss in petrogenesis, and argue that the heat for crustal fusion was convected by intruding mafic magmas.

### Regional geology

Before the break-up of Gondwana and the formation of the Weddell Sea, the Antarctic Peninsula was part of the proto-Pacific margin of the supercontinent. There is increasing evidence for pre-Mesozoic basement beneath parts of the magmatic arc. Granitic orthogneisses with early Palaeozoic ages are present in eastern Graham Land (Milne & Millar 1989) and NW Palmer Land (Harrison & Loske 1988; Harrison & Piercy 1991). The extent of the basement has not been clearly established in NE Palmer Land. The highly deformed nature of granitic orthogneisses and minor paragneisses prompted early workers to assume that they

were part of the pre-Mesozoic basement (e.g. Singleton 1980). Others (Pankhurst 1983; Meneilly *et al.* 1987; Wever *et al.* 1994) have suggested that few of these gneisses are Palaeozoic and that they are mainly plutonic rocks emplaced during early Mesozoic times and deformed during Late Jurassic or Early Cretaceous times.

Another suite of metasedimentary rocks in NE Palmer Land consists of argillites and metavolcaniclastic sandstones, known as the Mount Hill Formation (Singleton 1980), which are thought to have been deposited in a marginal back-arc basin (Suárez 1976). Associated volcanic rocks consist of a bimodal suite of mafic greenstones, which occur mainly as doleritic sills within the Mount Hill metasedimentary rocks, and a series of felsic metavolcanic rocks of the Brennecke Formation (Storey *et al.* 1987a) which have geochemical and isotopic features consistent with their formation in an extending back-arc basin (Wever & Storey 1992). Amphibolitic dykes are common within the granitic basement gneisses and are concordant with the regional westward-dipping foliation. These deformed dykes have isotopic and geochemical characteristics similar to the mafic greenstones and may be feeders to them. The metavolcanic and metasedimentary rocks have a westward-dipping cleavage and eastward-verging folds, which are related to a period of Late Jurassic to Early Cretaceous arc compression (Meneilly *et al.* 1987).

### Field relations and rock description

The gneisses crop out in a zone which extends northwards from Mount Jackson to Pinther Ridge and includes the Welch Mountains (Fig. 1). They form a westward-dipping association of sheared granitoids and migmatitic paragneisses. Most of the igneous rocks have a strong penetrative fabric related to eastward-directed ductile thrusting. Locally, the main foliation is cut by some steeper west-dipping shear zones with normal fault displacement.

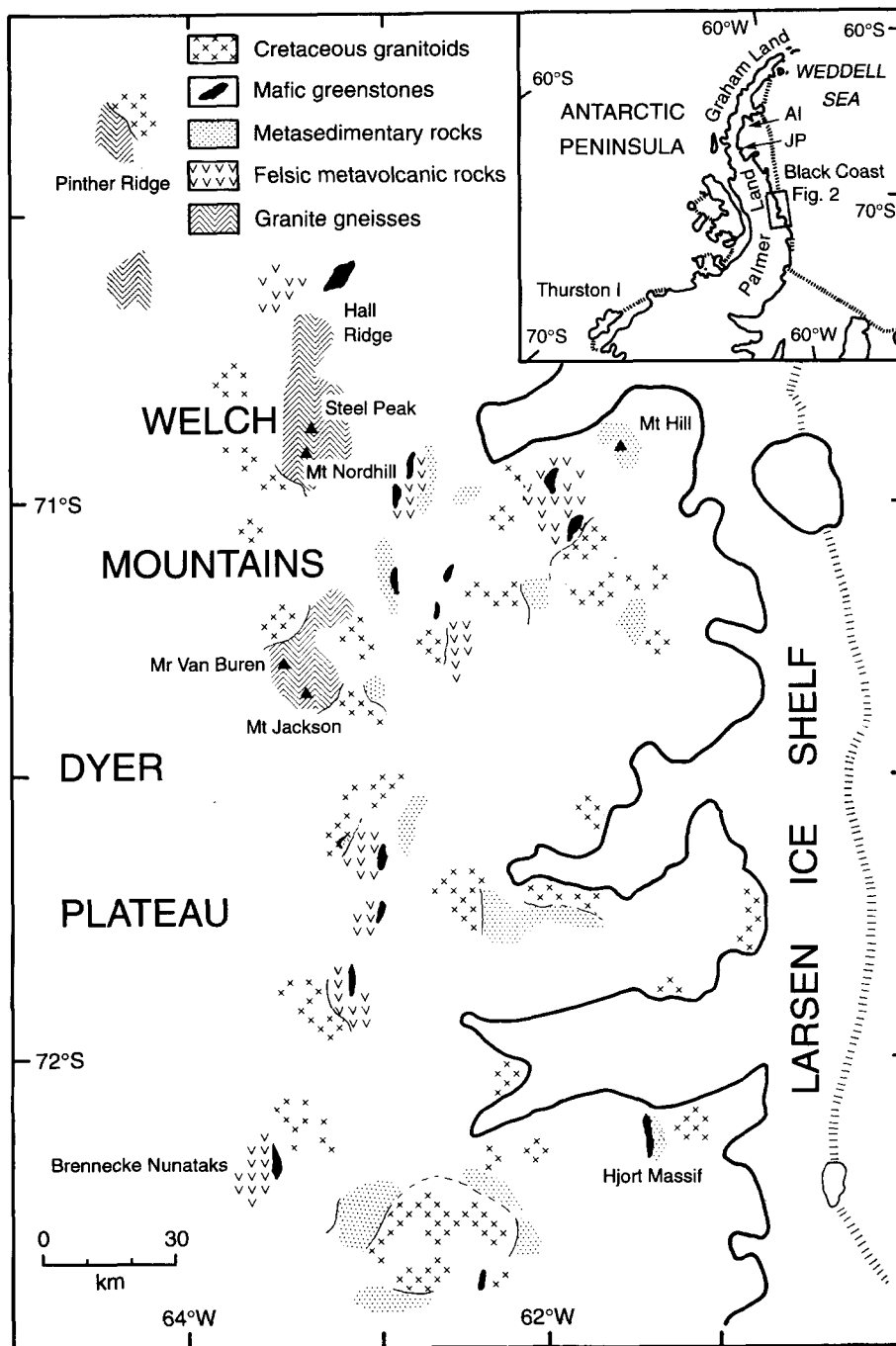


**Fig. 1.** Geological sketch map of the central Black Coast, NE Palmer Land; modified after Singleton (1980). Inset is a location map showing the study area situated along the eastern margin of N Palmer Land on the Antarctic Peninsula. JP, Joerg Peninsula; AI, Adie Inlet.

### *Mount Jackson and Mount Van Buren*

The dominant lithofacies at Mount Jackson and Mount Van Buren is a foliated porphyroclastic leucogranite, which occurs either as homogeneous orthogneiss or as sheared intrusive sheets within migmatitic paragneiss. The leucogranite forms the bulk of Mount Jackson and Mount Van Buren, but grades along its lower eastern flank into a westward-dipping migmatite complex consisting of quartzitic and semi-pelitic paragneiss, sheared granitic sheets, and subconcordant K-feldspar-rich pegmatites. C–S fabrics of the orthogneiss, stretching lineations, and sheath-folds

within the mylonitic quartzites are consistent with ENE-directed thrusting.

The leucogranites are protomylonites to orthomylonites according to the terminology of Wise *et al.* (1984). Porphyroclasts of feldspar (mainly K-feldspar) show undulatory extinction, shear fractures and mortar-texture, whereas the matrix grains show evidence for extensive recovery and recrystallization to finer-grained aggregates. The leucogranites are dominantly composed of perthitic orthoclase, quartz, plagioclase, and to a lesser extent biotite. The orthoclase phenocrysts are mostly 1 to 2 cm long and many show simple twinning. Muscovite is common,

but not ubiquitous. Some specimens contain coarse-grained muscovite of apparent magmatic origin; most have fine-grained muscovite which is secondary. The granite contains occasional garnet and/or sillimanite. Apatite, sparse zircon and uncommon opaque grains are the only conspicuous accessory phases.

### Welch Mountains

'Basement' lithologies from the eastern Welch Mountains consist of three different rock types: paragneiss, gneissic K-feldspar megacrystic granite, and homogeneous biotite-orthogneiss. These rocks are best exposed along the eastern flanks of Mount Nordhill and Steel Peak, where the higher ridges are formed by a foliated megacrystic granite which grades eastward into a sheeted complex resembling that of Mount Jackson. The complex consists of medium-grained paragneiss disrupted by granitic sheets and coarse-grained pegmatites. Garnet is common in the granitic sheets and the pegmatites, whereas it is sparse in the paragneisses which consist mainly of biotite, feldspar, quartz, and, in places, muscovite and sillimanite. The megacrystic granite cuts the paragneisses and locally contains schlieren of fine-grained biotite-gneiss and garnet-bearing pegmatitic segregations. It is a strongly porphyritic rock containing alkali-feldspar (microcline and perthitic orthoclase), quartz, plagioclase, biotite and accessory apatite, zircon and rutile. Muscovite, epidote and chlorite occur as minor secondary phases. Tabular K-feldspar phenocrysts are up to 6 cm in length, show simple twinning and occur in alignment with sheared folia of the matrix. The matrix has accommodated strain and generally displays a well-developed C-S fabric, whereas the phenocrysts behaved more rigidly. Deformation-related features like kinking (biotite), undulatory extinction and subgrain structures (quartz and plagioclase), and recrystallization are common within the matrix grains.

Biotite-orthogneisses are medium-grained, homogeneous rocks that locally contain biotite-rich xenoliths. They are broadly granodioritic in composition and consist dominantly of plagioclase, quartz, orthoclase and biotite, (locally replaced by chlorite and minor epidote). Titanite is relatively abundant, and other accessory phases include apatite, zircon and opaque grains. Garnet and tourmaline are present sporadically. The latter tends to be restricted to zones of more intense deformation. These foliated rocks exhibit a good C-S fabric defined by biotite alignment and folia of variably recrystallized quartz-feldspar aggregates. Porphyroclasts of plagioclase are common, partly altered to sericite. The field relations of the biotite-orthogneisses are not exposed.

### Pinther Ridge

Foliated granitoids from Pinther Ridge and Hall Ridge consist of a series of heterogeneous granitic to dioritic gneisses of which the majority are represented by a mildly porphyritic leucocratic granodiorite. The leucocratic gneisses contain locally disrupted layers and elongated pods of finer grained dioritic gneiss. The foliation dips moderately westward and is defined by a compositional layering concordant to a tectonic fabric. Schlieren of folded mafic material are common within the leucocratic layers. The granitic gneisses also show a distinct augen-like texture of fractured and partially recrystallized feldspar phenocrysts. The mineralogy of the leucocratic gneisses is dominated by plagioclase, alkali-feldspar, quartz and biotite. The mesocratic rocks consist mainly of plagioclase, amphibole, biotite, and minor quartz. Amphibole has cores of clinopyroxene in places. Accessory minerals are apatite, zircon, magnetite and allanite.

### Geochronology

Rb-Sr geochronological data and Nd values of the granitic gneisses are summarized in Table 1. The seven point Rb-Sr isochron for the Mount Van Buren leucogranite yields an age of  $206 \pm 3$  Ma. This is similar to the age of the Mount Jackson leucogranite and is interpreted as the age of magmatic crystallization. The megacrystic granite, biotite orthogneiss and foliated granitoids give less constrained results, but overlap in age with the Early Jurassic leucogranites (Table 1). The paragneisses (undated) may be much older. With the exception of the foliated granitoids from Pinther Ridge, all the granitic gneisses have high initial  $^{87}\text{Sr}/^{86}\text{Sr}$  ratios (0.7125–0.7210) and low  $\epsilon_{\text{Nd}}$  values (–7.4 to –9.4). These values imply a considerable input of ancient continental crust and indicate the presence of pre-Mesozoic basement in NE Palmer Land (Wever *et al.* 1994).

### Timing of deformation

The age relationships between Early Jurassic magmatism, deformation, and the formation or closure of the back-arc basin is uncertain as there are no absolute age constraints on the timing of deformation and formation of the gneissic fabrics. Meneilly *et al.* (1987) recognized within NE Palmer Land two periods of arc compression, one in the Early Jurassic and the other in the Late Jurassic to Early Cretaceous, which are separated by a period of arc and back-arc extension. They suggested that steep ductile faults, with downthrow towards the centre of the arc, affecting

**Table 1.** Summary of isotopic and geochronological data for early Mesozoic granitoids, NE Palmer Land

Location	Rock type	Age (Ma)	$^{87}\text{Sr}/^{86}\text{Sr}_i$	Points	MSWD	$\epsilon_{\text{Nd}}$
Mt Van Buren	Leucogranite	$206 \pm 3$	$0.7197 \pm 5$	7	2.7	–8.8
Mt Jackson	Leucogranite	$199 \pm 7$	$0.7210 \pm 1$	7	10.2	–9.4
Mt Nordhill	Megacrystic granite	$221 \pm 14$	$0.7125 \pm 7$	7	0.5	–7.4
Mt Nordhill	Biotite orthogneiss	$219 \pm 57$	$0.7156 \pm 28$	8	6.3	–7.9
Pinther Ridge	Foliated granitoid	$209 \pm 25$	$0.7058 \pm 2$	5	0.8	–3.4
Hall Ridge	Foliated granitoid	$211 \pm 70$	$0.7056 \pm 5$	5	7.8	–1.9

Full data presented by Wever *et al.* (1994).

Jurassic plutons and deformed mafic dykes represent Mid-Jurassic to mid-Cretaceous extensional faults, related to formation of the back-arc basin. However, this implies that the main foliation of the granitic gneisses predates the opening of the back-arc basin. If this is the case, then one would expect to observe within the granitic gneisses, a set of younger compressional structures corresponding to the Late Jurassic to Early Cretaceous deformation of the back-arc basin sedimentary rocks. These structures should affect both the main foliation and the normal ductile faults. But, the granitic gneisses show only one apparent set of compressional-related structures. It seems more likely to us that the main foliation of the gneisses is temporally related to the deformation of the back-arc sedimentary rocks. This would mean that deformation of the granitic gneisses postdates formation of the back-arc basin and does not require the Early Jurassic phase of arc compression of Meneilly *et al.* (1987).

Field relations of the deformed amphibolite dykes occurring within the granitic gneisses and the normal ductile faults are consistent with such an interpretation. The origin of these mafic dykes is probably related to extension during formation of the back-arc basin (Meneilly *et al.* 1987; Wever & Storey 1992). The dykes occur parallel to the main foliation and show minor, shear-related folds with eastward-vergence along their margins, indicating that they were emplaced prior to the main deformation. Some of the dykes are also discordant to and displaced by the normal faults (Meneilly *et al.* 1987). These relationships suggest that the extensional faults were not coeval with formation of the back-arc basin, but originated sometime after its closure, possibly in response to a period of either thermal relaxation or gravity-driven collapse.

In conclusion, we recognize two different structural regimes. The first produced the main foliation and was related to eastward-directed ductile thrusting during closure of the back-arc basin. The second produced a series of discrete, semi-ductile, extensional normal faults with downthrow to the west. These extensional faults are common in the granitic gneisses, but were not observed in Lower Cretaceous granitoids.

## Geochemistry

Major and trace element abundances on leucogranites, megacrystic granites, biotite-orthogneiss, foliated granitoids and paragneiss were determined using standard XRF methods at the University of Keele (Floyd 1985) on fused glass discs and pressed powder pellets respectively. Rare earth element (REE) Sc, Ta, Th and Hf abundances were determined on a subset of samples by instrumental neutron activation analysis (INAA) at the Open University (Potts 1987). A representative set of data is given in Table 2. Sr and Nd isotopic data are presented by Wever *et al.* (1994).

The samples are silicic, with only some of the foliated granodiorites having <65 wt% SiO<sub>2</sub>. All samples, except the foliated granitoids, are potassic (K<sub>2</sub>O > Na<sub>2</sub>O). The aluminous character of the suite is shown in Fig. 2. The samples have higher Al/(Na + K + Ca) ratios, at similar SiO<sub>2</sub> abundances, compared with dominantly metaluminous, West Antarctic, magmatic arc plutonic rocks from W Graham Land, W Palmer Land, and Thurston Island. The leucogranites have a small range in silica contents, and are distinctly peraluminous, trending toward paragneiss com-

positions. The magmatic trend of increasing Al/(Na + K + Ca) with increasing SiO<sub>2</sub> and aluminous index in the magmatic arc rocks is mainly a result of fractional crystallization, which can yield mildly peraluminous silicic magmas (Leat *et al.* 1993). But the strongly peraluminous composition of the leucogranites suggests they represent partial melts of peraluminous continental crust, similar to that represented by the paragneisses (Fig. 2). The trace element characteristics of the leucogranites also suggest generation by crustal partial fusion. For example, they have relatively high Rb/Zr ratios of 2.5–3.0, which are comparable to those of syn-continental collision granites, whereas the rest of the suite has lower Rb/Zr ratios (0.3–2.0), similar to those of volcanic arc granites (Harris *et al.* 1986). All samples are LREE enriched (Fig. 3), and have similar LREE and MREE patterns, except that the leucogranites have relatively low LREE-MREE abundances. The leucogranites and megacrystic granites are distinct in having the lowest HREE abundances, and the largest negative Eu anomalies. In Fig. 4, all granitoids are enriched in LILE relative to HFSE. The leucogranites and megacrystic granites have high Rb abundances and high Rb/Ba ratios relative to the other rocks. Jurassic felsic volcanic rocks of the Brennecke Formation are chemically similar to the biotite orthogneisses.

## Isotopic constraints

An extreme range in isotopic composition is established by samples from this study (Fig. 5). The paragneisses, having <sup>87</sup>Sr/<sup>86</sup>Sr<sub>200</sub> ratios of 0.7248–0.7265, (Wever *et al.* 1994) have the most radiogenic Sr known from the Antarctic Peninsula. Moreover, the plutonic samples with the exception of the foliated granodiorites, have higher initial <sup>87</sup>Sr/<sup>86</sup>Sr ratios than published values from Graham Land plutonic rocks. The samples form a trend of strongly increasing <sup>87</sup>Sr/<sup>86</sup>Sr with weakly decreasing <sup>143</sup>Nd/<sup>144</sup>Nd. Two petrogenetic mixing curves in Fig. 5 model this trend by mixing of basalt and partial melt of paragneiss. Curve A models mixing of MORB with partial melt generated from the paragneiss. MORB, or closely related basalt, has been widely suggested as a major component in mafic magma supply to arcs and back arc basins (Ewart & Hawkesworth 1987; Hildreth & Moorbath 1988; McCulloch & Gamble 1991). The trajectory of this curve lies well away from the samples in Fig. 5, however, and depleted basalt was clearly not important in the evolution of these rocks. Curve B models mixing of a more enriched basalt (at the low <sup>143</sup>Nd/<sup>144</sup>Nd end of the MORB-OIB range) with the crustal composition. The basalt is one of the Jurassic Kirwan basalt lavas from Dronning Maud Land, Antarctica (Harris *et al.* 1990), which form part of the flood basalt province associated with the rifting of Africa from Antarctica during Gondwana break-up (Storey *et al.* 1992; Brewer *et al.* 1992). The Kirwan basalts chemically resemble contemporaneous Karoo lavas of southern Africa, but are distinct from Jurassic Ferrar Supergroup flood basalts in Antarctica (Harris *et al.* 1990; Hergt *et al.* 1989). Curve B is a close fit to the Palmer Land data (Fig. 5), suggesting that the rocks were generated by mixing of basalt magma and partial melt derived from the paragneiss in various proportions, although subsequent fractional crystallization modified bulk composition. The foliated granitoids plot close to the basaltic end member, and the crustal contribution to these samples was likely

**Table 2. Geochemical analyses of paragneisses and Jurassic granitoids, NE Palmer Land**

Sample	Leucogranites										Megacrystic granites										Biotite-orthogneisses										Foliated granitoids										Paragneisses																																																											
	R.2109.2	R.2109.8	R.4908.12	R.4908.10	R.4920.10	R.4920.12	R.4294.4	R.4552.9	R.4552.2	R.4906.6	R.4921.1	R.4921.4	R.5006.1	R.5006.7	R.5010.13	R.4942.4	R.4294.1	R.4293.1	R.4920.8	R.4293.2	R.2109.2	R.2109.8	R.4908.12	R.4908.10	R.4920.10	R.4920.12	R.4294.4	R.4552.9	R.4552.2	R.4906.6	R.4921.1	R.4921.4	R.5006.1	R.5006.7	R.5010.13	R.4942.4	R.4294.1	R.4293.1	R.4920.8	R.4293.2	R.2109.2	R.2109.8	R.4908.12	R.4908.10	R.4920.10	R.4920.12	R.4294.4	R.4552.9	R.4552.2	R.4906.6	R.4921.1	R.4921.4	R.5006.1	R.5006.7	R.5010.13	R.4942.4	R.4294.1	R.4293.1	R.4920.8	R.4293.2	R.2109.2	R.2109.8	R.4908.12	R.4908.10	R.4920.10	R.4920.12	R.4294.4	R.4552.9	R.4552.2	R.4906.6	R.4921.1	R.4921.4	R.5006.1	R.5006.7	R.5010.13	R.4942.4	R.4294.1	R.4293.1	R.4920.8	R.4293.2																				
SiO <sub>2</sub>	72.66	73.64	71.82	71.80	68.19	69.52	67.74	71.84	69.70	69.36	65.80	69.99	61.15	65.20	58.23	59.12	70.03	74.98	73.17	75.05	72.66	73.64	71.82	71.80	68.19	69.52	67.74	71.84	69.70	69.36	65.80	69.99	61.15	65.20	58.23	59.12	70.03	74.98	73.17	75.05	72.66	73.64	71.82	71.80	68.19	69.52	67.74	71.84	69.70	69.36	65.80	69.99	61.15	65.20	58.23	59.12	70.03	74.98	73.17	75.05	72.66	73.64	71.82	71.80	68.19	69.52	67.74	71.84	69.70	69.36	65.80	69.99	61.15	65.20	58.23	59.12	70.03	74.98	73.17	75.05	72.66	73.64	71.82	71.80	68.19	69.52	67.74	71.84	69.70	69.36	65.80	69.99	61.15	65.20	58.23	59.12	70.03	74.98	73.17	75.05
TiO <sub>2</sub>	0.23	0.18	0.28	0.30	0.59	0.69	0.67	0.32	0.84	0.84	1.35	0.85	0.80	0.63	0.83	0.66	1.04	0.72	1.01	0.71	0.23	0.18	0.28	0.30	0.59	0.69	0.67	0.32	0.84	0.84	1.35	0.85	0.80	0.63	0.83	0.66	1.04	0.72	1.01	0.71	0.23	0.18	0.28	0.30	0.59	0.69	0.67	0.32	0.84	0.84	1.35	0.85	0.80	0.63	0.83	0.66	1.04	0.72	1.01	0.71	0.23	0.18	0.28	0.30	0.59	0.69	0.67	0.32	0.84	0.84	1.35	0.85	0.80	0.63	0.83	0.66	1.04	0.72	1.01	0.71	0.23	0.18	0.28	0.30	0.59	0.69	0.67	0.32	0.84	0.84	1.35	0.85	0.80	0.63	0.83	0.66	1.04	0.72	1.01	0.71
Al <sub>2</sub> O <sub>3</sub>	14.36	14.53	14.84	14.73	15.06	14.80	14.94	14.78	13.10	12.90	13.35	13.19	18.19	16.86	17.88	17.64	13.25	12.68	12.32	11.20	14.36	14.53	14.84	14.73	15.06	14.80	14.94	14.78	13.10	12.90	13.35	13.19	18.19	16.86	17.88	17.64	13.25	12.68	12.32	11.20	14.36	14.53	14.84	14.73	15.06	14.80	14.94	14.78	13.10	12.90	13.35	13.19	18.19	16.86	17.88	17.64	13.25	12.68	12.32	11.20	14.36	14.53	14.84	14.73	15.06	14.80	14.94	14.78	13.10	12.90	13.35	13.19	18.19	16.86	17.88	17.64	13.25	12.68	12.32	11.20	14.36	14.53	14.84	14.73	15.06	14.80	14.94	14.78	13.10	12.90	13.35	13.19	18.19	16.86	17.88	17.64	13.25	12.68	12.32	11.20
Fe <sub>2</sub> O <sub>3</sub>	1.58	1.36	1.80	1.84	3.04	2.92	3.30	1.71	5.67	6.61	7.49	5.68	5.19	4.14	6.73	7.10	6.07	1.86	4.99	4.19	1.58	1.36	1.80	1.84	3.04	2.92	3.30	1.71	5.67	6.61	7.49	5.68	5.19	4.14	6.73	7.10	6.07	1.86	4.99	4.19	1.58	1.36	1.80	1.84	3.04	2.92	3.30	1.71	5.67	6.61	7.49	5.68	5.19	4.14	6.73	7.10	6.07	1.86	4.99	4.19	1.58	1.36	1.80	1.84	3.04	2.92	3.30	1.71	5.67	6.61	7.49	5.68	5.19	4.14	6.73	7.10	6.07	1.86	4.99	4.19	1.58	1.36	1.80	1.84	3.04	2.92	3.30	1.71	5.67	6.61	7.49	5.68	5.19	4.14	6.73	7.10	6.07	1.86	4.99	4.19
MnO	0.03	0.03	0.03	0.03	0.03	0.03	0.04	0.01	0.09	0.10	0.11	0.09	0.08	0.06	0.11	0.13	0.12	0.05	0.08	0.11	0.03	0.03	0.03	0.03	0.03	0.03	0.04	0.01	0.09	0.10	0.11	0.09	0.08	0.06	0.11	0.13	0.12	0.05	0.08	0.11	0.03	0.03	0.03	0.03	0.03	0.03	0.04	0.01	0.09	0.10	0.11	0.09	0.08	0.06	0.11	0.13	0.12	0.05	0.08	0.11	0.03	0.03	0.03	0.03	0.03	0.03	0.04	0.01	0.09	0.10	0.11	0.09	0.08	0.06	0.11	0.13	0.12	0.05	0.08	0.11																				
MgO	0.33	0.10	0.31	0.35	1.18	1.29	1.40	0.42	1.02	0.70	1.90	1.06	1.82	1.44	3.45	3.11	2.34	0.33	1.67	1.23	0.33	0.10	0.31	0.35	1.18	1.29	1.40	0.42	1.02	0.70	1.90	1.06	1.82	1.44	3.45	3.11	2.34	0.33	1.67	1.23	0.33	0.10	0.31	0.35	1.18	1.29	1.40	0.42	1.02	0.70	1.90	1.06	1.82	1.44	3.45	3.11	2.34	0.33	1.67	1.23	0.33	0.10	0.31	0.35	1.18	1.29	1.40	0.42	1.02	0.70	1.90	1.06	1.82	1.44	3.45	3.11	2.34	0.33	1.67	1.23																				
CaO	0.74	0.68	0.86	0.89	2.09	2.12	2.25	1.02	2.46	2.46	4.13	2.51	5.37	3.46	5.91	6.62	1.14	0.60	1.23	1.56	0.74	0.68	0.86	0.89	2.09	2.12	2.25	1.02	2.46	2.46	4.13	2.51	5.37	3.46	5.91	6.62	1.14	0.60	1.23	1.56	0.74	0.68	0.86	0.89	2.09	2.12	2.25	1.02	2.46	2.46	4.13	2.51	5.37	3.46	5.91	6.62	1.14	0.60	1.23	1.56	0.74	0.68	0.86	0.89	2.09	2.12	2.25	1.02	2.46	2.46	4.13	2.51	5.37	3.46	5.91	6.62	1.14	0.60	1.23	1.56																				
Na <sub>2</sub> O	2.84	3.24	2.68	2.68	2.69	2.89	3.05	2.80	2.70	2.28	2.13	1.94	2.30	4.32	4.22	4.17	2.78	1.80	1.69	2.12	2.84	3.24	2.68	2.68	2.69	2.89	3.05	2.80	2.70	2.28	2.13	1.94	2.30	4.32	4.22	4.17	2.78	1.80	1.69	2.12	2.84	3.24	2.68	2.68	2.69	2.89	3.05	2.80	2.70	2.28	2.13	1.94	2.30	4.32	4.22	4.17	2.78	1.80	1.69	2.12	2.84	3.24	2.68	2.68	2.69	2.89	3.05	2.80	2.70	2.28	2.13	1.94	2.30	4.32	4.22	4.17	2.78	1.80	1.69	2.12																				
K <sub>2</sub> O	5.42	5.10	6.09	6.10	5.28	4.77	4.95	5.81	3.86	3.85	2.64	3.85	1.68	3.06	2.24	2.31	3.22	6.01	2.28	3.02	5.42	5.10	6.09	6.10	5.28	4.77	4.95	5.81	3.86	3.85	2.64	3.85	1.68	3.06	2.24	2.31	3.22	6.01	2.28	3.02	5.42	5.10	6.09	6.10	5.28	4.77	4.95	5.81	3.86	3.85	2.64	3.85	1.68	3.06	2.24	2.31	3.22	6.01	2.28	3.02	5.42	5.10	6.09	6.10	5.28	4.77	4.95	5.81	3.86	3.85	2.64	3.85	1.68	3.06	2.24	2.31	3.22	6.01	2.28	3.02																				
P <sub>2</sub> O <sub>5</sub>	0.32	0.33	0.38	0.37	0.37	0.42	0.41	0.29	0.21	0.31	0.45	0.22	0.26	0.19	0.23	0.22	0.09	0.01	0.11	0.40	0.32	0.33	0.38	0.37	0.37	0.42	0.41	0.29	0.21	0.31	0.45	0.22	0.26	0.19	0.23	0.22	0.09	0.01	0.11	0.40	0.32	0.33	0.38	0.37	0.37	0.42	0.41	0.29	0.21	0.31	0.45	0.22	0.26	0.19	0.23	0.22	0.09	0.01	0.11	0.40	0.32	0.33	0.38	0.37	0.37	0.42	0.41	0.29	0.21	0.31	0.45	0.22	0.26	0.19	0.23	0.22	0.09	0.01	0.11	0.40																				
LOI	0.85	0.71	0.36	0.37	0.97	0.49	1.01	0.96	0.47	0.96	0.92	0.57	0.64	0.30	0.61	0.67	1.12	0.83	1.21	0.73	0.85	0.71	0.36	0.37	0.97	0.49	1.01	0.96	0.47	0.96	0.92	0.57	0.64	0.30	0.61	0.67	1.12	0.83	1.21	0.73	0.85	0.71	0.36	0.37	0.97	0.49	1.01	0.96	0.47	0.96	0.92	0.57	0.64	0.30	0.61	0.67	1.12	0.83	1.21	0.73	0.85	0.71	0.36	0.37	0.97	0.49	1.01	0.96	0.47	0.96	0.92	0.57	0.64	0.30	0.61	0.67	1.12	0.83	1.21	0.73																				
Total	99.36	99.90	99.53	99.47	99.69	100.12	99.50	99.89	99.69	100.21	100.38	100.32	99.50	99.56	100.38	100.35	100.23	99.80	100.17	99.99	99.36	99.90	99.53	99.47	99.69	100.12	99.50	99.89	99.69	100.21	100.38	100.32	99.50	99.56	100.38	100.35	100.23	99.80	100.17	99.99	99.36	99.90	99.53	99.47	99.69	100.12	99.50	99.89	99.69	100.21	100.38	100.32	99.50	99.56	100.38	100.35	100.23	99.80	100.17	99.99	99.36	99.90	99.53	99.47	99.69	100.12	99.50	99.89	99.69	100.21	100.38	100.32	99.50	99.56	100.38	100.35	100.23	99.80	100.17	99.99																				
Rb	320	399	331	337	297	299	251	303	180	170	166	179	71	95	87	78	149	267	145	268	320	399	331	337	297	299	251	303	180	170	166	179	71	95	87	78	149	267	145	268	320	399	331	337	297	299	251	303	180	170	166	179	71	95	87	78	149	267	145	268	320	399	331	337	297	299	251	303	180	170	166	179	71	95	87	78	149	267	145	268																				
Sr	87	60	109	109	243	223	277	115	159	160	147	149	657	464	658	478	187	144	224	113	87	60	109	109	243	223	277	115	159	160	147	149	657	464	658	478	187	144	224	113	87	60	109	109	243	223	277	115	159	160	147	149	657	464	658	478	187																																											

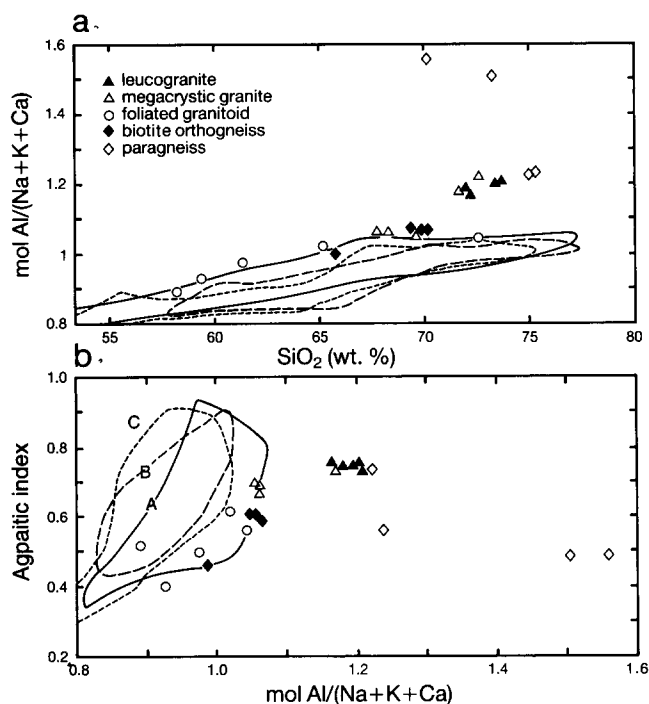


**Fig. 2.** (a) Aluminum saturation (molecular Al/(Na + K + Ca)) vs. SiO<sub>2</sub> and (b) agpaitic index (molecular (Na + K)/Al) for NE Palmer Land samples. The fields are for subduction-related Mesozoic–Cenozoic plutonic suites from West Antarctica, (A) Thurston Island (Leat *et al.* 1993), (B) W Palmer Land (Harrison & Piercy 1990) and (C) W Graham Land (Group I plutons, Hole 1986).

<10%. The megacrystic granites and orthogneisses can be modelled by approximately 50–70% contamination of basalt by crust, and the leucogranites represent over 75% crustal end-member. We note that these percentages depend on two factors.

(1) *Crustal composition.* The composition of the paragneiss involved in petrogenesis may differ from the exposed and sampled paragneiss. The three sampled paragneisses range in <sup>87</sup>Sr/<sup>86</sup>Sr<sub>200</sub> from 0.7248 to 0.7265 (Wever *et al.* 1994), all significantly more radiogenic (Fig. 5) than the highest <sup>87</sup>Sr/<sup>86</sup>Sr leucogranite (0.7208). It is likely that the potential source of the leucogranites is compositionally more varied than the range of the sampled paragneisses, and it is likely that a less radiogenic parent paragneiss partially-melted to form the leucogranites without mixing with basalt.

(2) *Generation of the silicic end member.* The mixing is likely to have taken place between basalt and a leucogranite end member melt, with the same Sr and Nd isotope ratios as the paragneiss parent, but different trace element abundances, as modelled in Fig. 5. Nevertheless, some contamination of the basaltic magmas could have occurred by bulk assimilation of paragneiss. Modelling of magma generation by this process does not greatly change the trajectories of the mixing curves in Fig. 5.

Our model for the petrogenesis of the Palmer Land granitoids, based on Fig. 5, is as follows. (i) Partial melting of paragneiss to generate a leucogranite end member magma. (ii) Mixing of basalt magma from an enriched mantle source in various proportions with this silicic end

member magma to generate the megacrystic granites, and orthogneisses. (iii) Fractional crystallization of mafic magma, with less than 10% contamination by leucogranite or paragneiss, to generate the foliated granitoids. The simultaneous availability of basalt and leucogranite suggests that heat convected by the basaltic magma was responsible for partial fusion of the paragneisses. We envisage a situation similar to that discussed by Huppert & Sparks (1988) in which the mafic magma forms hypabyssal intrusions, and heat convected by the mafic magma partially melts the silicic country rocks. In the case of sills, mixing may not occur between mafic magma and partially melted crust in the intrusion roof (Huppert & Sparks 1988).

#### *Trace element modelling of petrogenetic trends*

Rb/Sr ratios of the granitoid samples increase with decreasing Sr and Ba abundances (Fig. 6), and such trends could result from fractional crystallization of alkali feldspar-dominated assemblages. Similar trends would also be generated by vapour-absent biotite or muscovite partial melting of the paragneisses to generate the leucogranites. (cf. Harris & Inger 1992; Inger & Harris 1993). Because the granites are alkali feldspar-phyric, the relative importance of these processes can probably not be decided. Nevertheless, the positive relationship between Ba and Rb/Sr in Fig. 6 suggests a role for biotite-dominated fractional crystallization in those rocks. Relationships in Fig. 7 are consistent with generation of the leucogranites by partial melting of the paragneisses. The leucogranites and the megacrystic granites, have higher Rb, but lower Y than the paragneisses, and could have been derived from them by partial melting with refractory garnet. The foliated granitoids and biotite orthogneisses have compositions consistent with generation by fractional crystallization of magmas generated by mixing of basalt and leucogranite. The leucogranites have significantly higher Rb/Th ratios than the other granitoids and the paragneisses. Generation of the leucogranites cannot be modelled by fractional crystallization of a feldspar, biotite and garnet assemblage from any of the other magmas, or by partial melting of paragneiss containing these minerals. But the high Rb/Th ratios of the leucogranites could result from fractional crystallization or partial melting if a Th-bearing mineral was a phenocryst or restite phase respectively. A likely candidate is monazite, which Rapp *et al.* (1987) argued can be a restite phase during generation of peraluminous magmas by crustal partial melting. Watt & Harley (1993) further argued that certain peraluminous leucogneisses from East Antarctica were generated by crustal partial melting involving monazite as a restite phase, generating low Th melts (their Type 1) comparable to the NE Palmer Land leucogranites.

#### **Discussion**

Studies of the petrogenesis of Mesozoic to early Tertiary Antarctic Peninsula igneous rocks constrained by isotopic data have favoured the view that the range of observed compositions is a result of mixing processes between mantle-derived basalt and silicic crust (Pankhurst *et al.* 1988; Hole *et al.* 1991). Such studies have been hampered, however, by insufficient knowledge of either the mantle or crustal-derived end member compositions. Our model for the petrogenesis of the gneisses from NE Palmer Land is

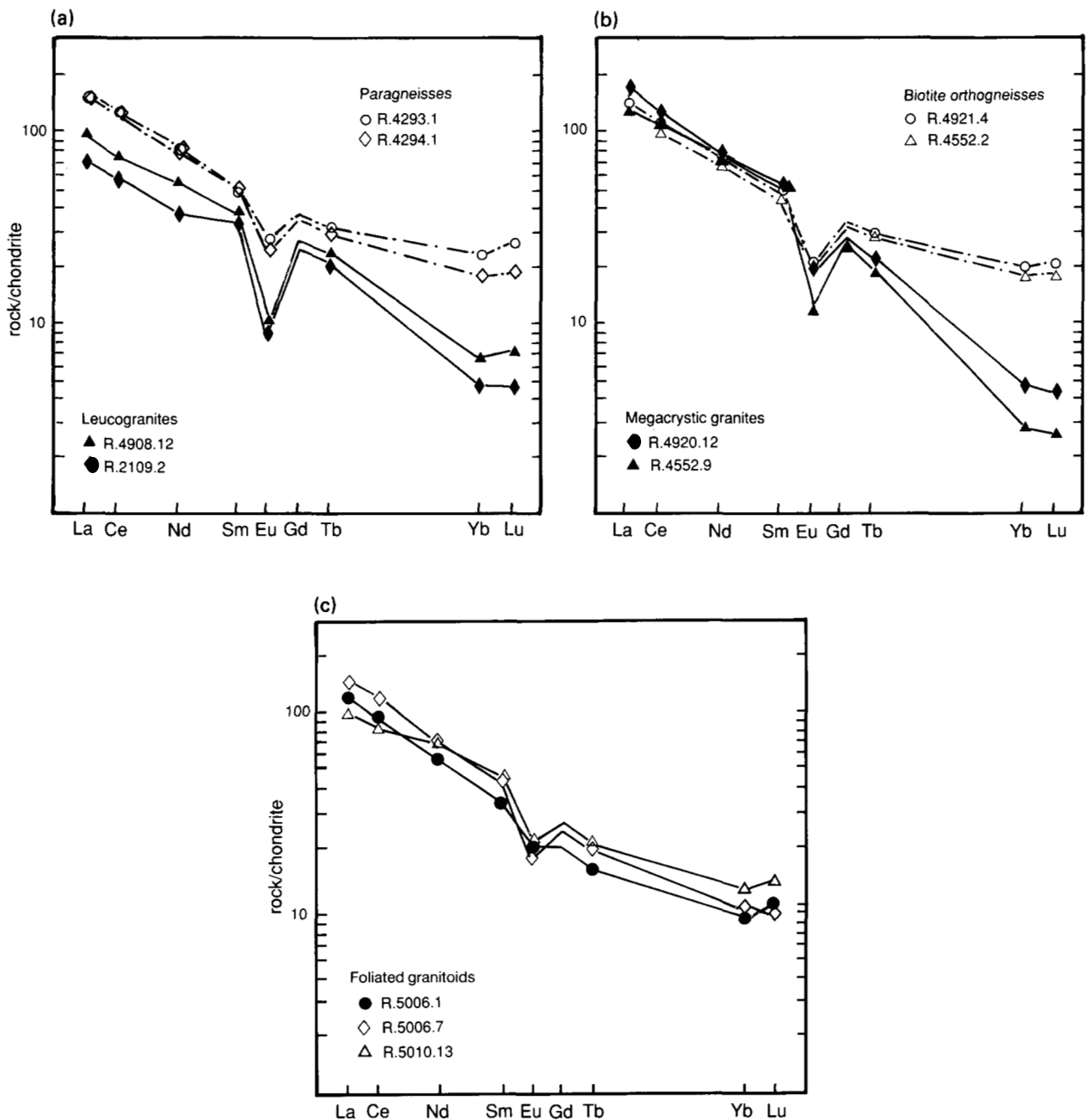


**Fig. 3.** Chondrite-normalized rare earth element patterns. (a) Leucogranites from Mount Van Buren and Mount Jackson and their possible source paragneisses. (b) K-feldspar megacrystic granites from the Welch Mountains and biotite-orthogneisses. (c) Foliated granitoids from Pinther Ridge.

similarly based on mixing of mafic and silicic magmas, but the compositions of the end-members (Fig. 5) are very different from those used by Pankhurst *et al.* (1988) and Hole *et al.* (1991).

#### Mafic end member

The basaltic end member composition we use has an initial  $^{143}\text{Nd}/^{144}\text{Nd}$  ratio (0.512418;  $t = 172$ ; Harris *et al.* 1990) within the range of Jurassic basalts from NE Palmer Land (0.512135–0.512575;  $t = 150$ ; Wever & Storey 1992). This

composition is distinct from those of the two other basalt types thought to have been present during the Jurassic–Tertiary evolution of the Antarctic Peninsula. (i) Basalt with Nd and Sr isotopic ratios similar to MORB believed to represent the mantle-derived end member in granitoid petrogenesis in Graham Land (Hole 1986; Pankhurst *et al.* 1988; Hole *et al.* 1991). (ii) Ferrar-like basalt having low initial  $^{143}\text{Nd}/^{144}\text{Nd}$  ratios of *c.* 0.51210–0.51224, erupted in great volume during the Jurassic in the Transantarctic Mountains (Hergt *et al.* 1989). Storey & Alabaster (1991) suggested that Ferrar-type basalt was present in northern

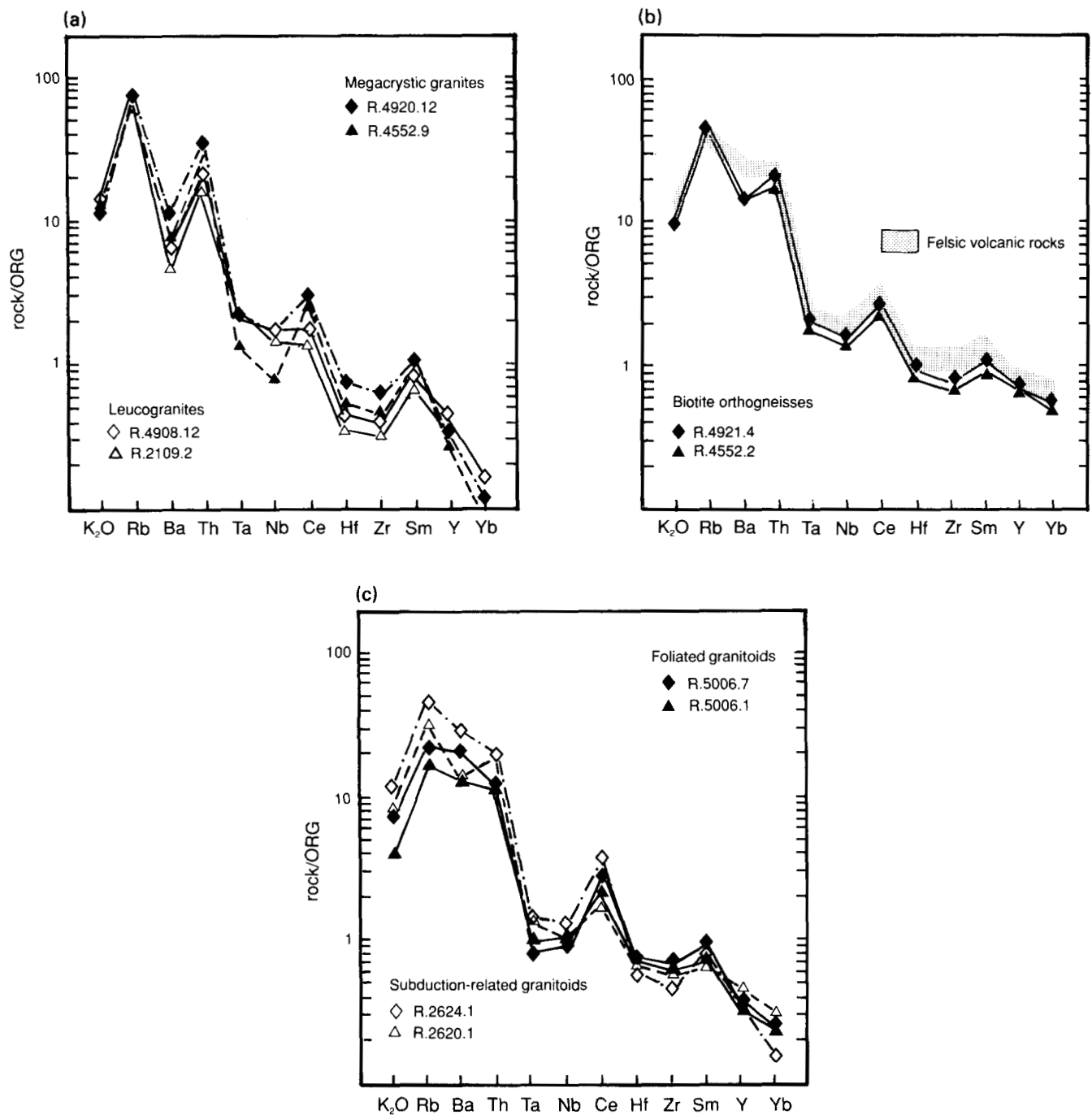


**Fig. 4.** Ocean ridge granite (ORG)-normalized multi-element diagrams after Pearce *et al.* 1984. (a) Leucogranites and megacrystic granites. (b) Biotite orthogneisses, with the field for felsic volcanic rocks of the Brennecke Formation (Wever & Storey 1992) for comparison. (c) Foliated granitoids from Pinter Ridge, with patterns of subduction-related granitoids from SE Graham Land (Hole 1986) for comparison.

Graham Land during Jurassic times. But there are few data with which to assess the distribution of different types of mafic magma with time during the evolution of the Antarctic Peninsula. The low  $^{143}\text{Nd}/^{144}\text{Nd}$  mafic magma we identify as an Early Jurassic end member in NE Palmer Land may be asthenospheric in origin, related to the Karoo mantle plume, or may represent partial melt of lithospheric mantle, or may contain components from both these sources.

#### *Silicic end member*

The paragneisses used as the crustal end-member in this paper have the highest known initial  $^{87}\text{Sr}/^{86}\text{Sr}$  ratios in the Antarctic Peninsula. They are significantly more  $^{87}\text{Sr}$ -enriched than the Adie Inlet gneisses, which have the highest known initial  $^{87}\text{Sr}/^{86}\text{Sr}$  ratios in Graham Land. Hole *et al.* (1991) used the Adie Inlet gneisses as crustal

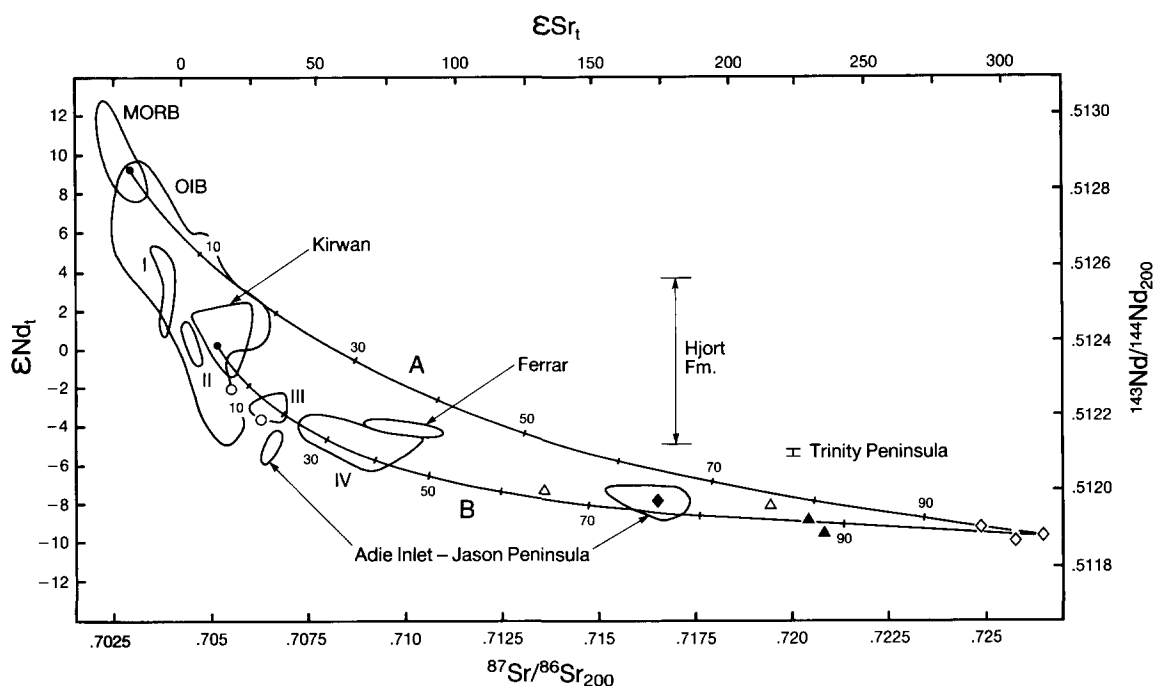


**Fig. 5.**  $\epsilon_{Nd_t}$  versus  $\epsilon_{Sr_t}$  plot for NE Palmer Land, with equivalent  $^{87}Sr/^{86}Sr$  and  $^{143}Nd/^{144}Nd$  values at 200 Ma (for  $^{143}Nd/^{144}Nd = 0.7219$ ). Symbols as in Fig. 2. The crust end member for the mixing curves is a partial melt of paragneiss having isotopic ratios of paragneiss R.4294.1 (Wever *et al.* 1993) and average leucogranite abundances of Sr (80 ppm) and Nd (28.5 ppm). The MORB end member is sample 104-16 (Sun & McDonough 1989), and the Kirwan basalt end member is sample LAG31. This sample and field for Kirwan basalts from Harris *et al.* (1990). Mixing curves A and B are marked with percent contamination of basalt with crust. MORB and OIB fields after Staudigel *et al.* (1984), Ferrar field after Hergt *et al.* 1989, Graham Land granitoid pluton groups I-IV and Adie Inlet-Jason Peninsula gneisses after Hole (1986) and Hole *et al.* (1991). The ranges in  $\epsilon_{Nd}$  in Hjort Formation basalts (Wever & Storey 1992) and Jurassic lavas from Trinity Peninsula, northern Graham Land (Storey & Alabaster 1991) are also shown.

end-member in their crust-basalt mixing models for the generation of Graham Land plutonic rocks. The implication is that there is a significant difference in crustal radiogenic isotopic composition between the E Graham Land and NE Palmer Land parts of the Antarctic Peninsula, so that models for the generation of the Mesozoic to Cenozoic igneous rocks must treat each part of the Antarctic Peninsula as a separate isotopic system.

### Tectonic implications

Hole *et al.* (1991) suggested that the extent of interaction between basalt and crust in the Antarctic Peninsula magmatic arc was mainly dependent on the crustal thickness. Pankhurst *et al.* (1988) proposed that crustal involvement within Andean granitoids was predominantly controlled by the style of subduction. They argued that during Triassic to Jurassic times a 'Chilean' type of shallow-dipping subduction underneath the peninsula would explain the relative large degree of crustal reactivation. In this model the margin would have been compressional, and the Late Triassic to Early Jurassic granitoids could be part of the pre-Andean Gondwanian orogen that was responsible for folding the Permian and older foreland basin sequences of the Cape and Ellsworth mountains fold belts (Storey *et al.* 1987b). This would be consistent with the Early Jurassic compressional phase recognized by Meneilly *et al.* 1987. But the NE Palmer Land Early Jurassic intrusive rocks are exposed along the margins of the back-arc basin system infilled with Middle and Upper Jurassic sedimentary rocks.

Together with the lack of field evidence for the Early Jurassic compressional event, this suggests that the crustal melting was associated with lithospheric attenuation along the Antarctic Peninsula margin. Silicic volcanic rocks, comparable to the peraluminous granitoids (Fig. 5) flank the marginal basin system and may represent their extrusive equivalents (Wever & Storey 1992). They are part of a bimodal sequence, the basaltic end-members of which may have formed by decompression mantle melting during lithospheric extension. The back-arc basin was deformed during a major compressional event prior to emplacement of post-tectonic Cretaceous calc-alkaline granites (Vennum & Rowley 1986). This may reflect changes in subduction zone parameters and eastward migration of arc magmatism into the back-arc region. The apparent restricted occurrence of crustal-derived granitoids to an arc-parallel belt of intense Late Jurassic to Early Cretaceous deformation suggests that crustal anatexis was related to a zone of major crustal failure which was reactivated during the deformation of the back-arc basin. Such a zone of structural weakness would be a highly feasible site for the generation of crustal-dominated magmatic rocks.

The crustal-derived granitoids are not restricted to the eastern margin of the Antarctic Peninsula but form part of a larger belt of Late Triassic and Jurassic magmatism along the proto-Pacific margin of Gondwana. In the adjoining Thurston Island crustal block of West Antarctica (Fig. 1) the single known Early Jurassic pluton is a mildly peraluminous two-mica granite, whose relatively high initial  $^{87}Sr/^{86}Sr$  ratio (0.710) and low  $\epsilon_{Nd_t}$  values (-5.6 and -6.8) (Pankhurst *et*

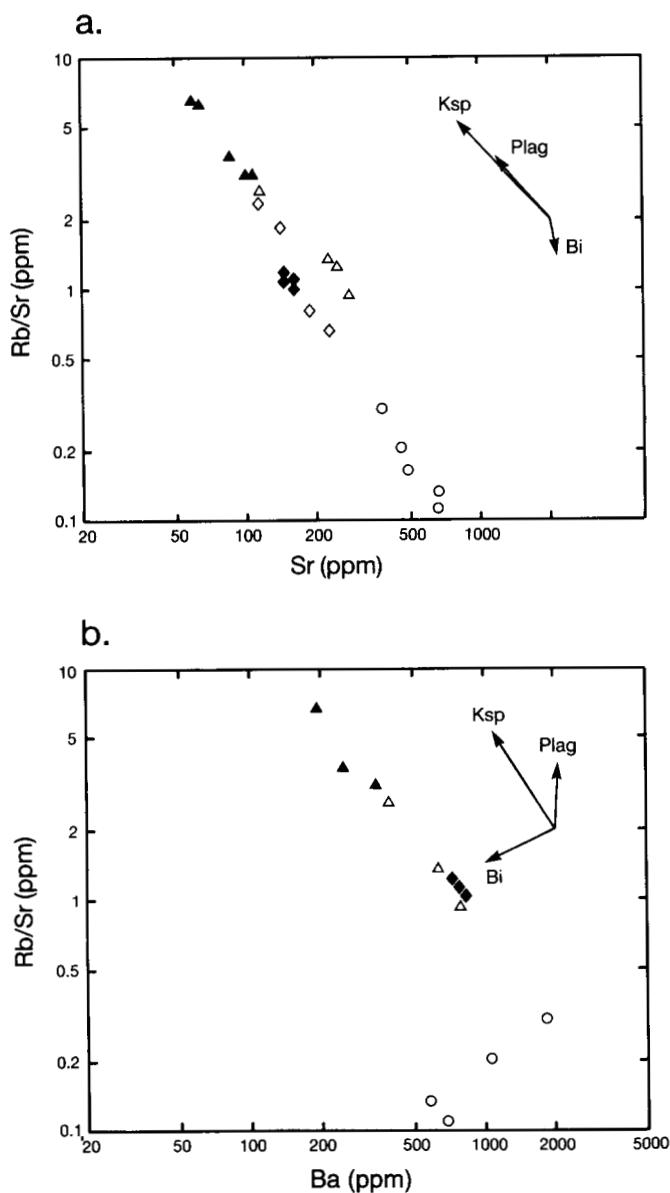


**Fig. 6.** Plots of Sr and Ba versus Rb/Sr for NE Palmer Land samples, symbols as in Fig. 2. Vectors for fractional crystallization are after the Rayleigh law for  $f = 0.9$ . Distribution coefficients selected from Henderson (1982).

*al.* 1993) indicate a significant crustal component. In southern South America *c.* 200 Ma calc-alkaline granitoids with moderate initial  $^{87}\text{Sr}/^{86}\text{Sr}$  ratios, so-called 'modified I types' (Pankhurst 1990) or 'transitional' granitoids (Parada 1990), are known from the Coast Ranges of central Chile (Parada *et al.* 1988) and from the North Patagonian Massif (Rapela *et al.* 1992). Triassic calc-alkaline and alkaline volcanic rocks in western Argentina are associated with rifting and formation of extensional basins (Gust *et al.* 1985; Uliana *et al.* 1989). Volcanism and extension continued during Middle and Late Jurassic times with formation of the extensive silicic Chon-Aike/Tobífera province (155–165 Ma, Gust *et al.* 1985) which, according to Bruhn *et al.* (1978), formed by crustal anatexis. Storey & Alabaster (1991) argued that at least part of this province was a product of either differentiation of an enriched mantle source or crustal

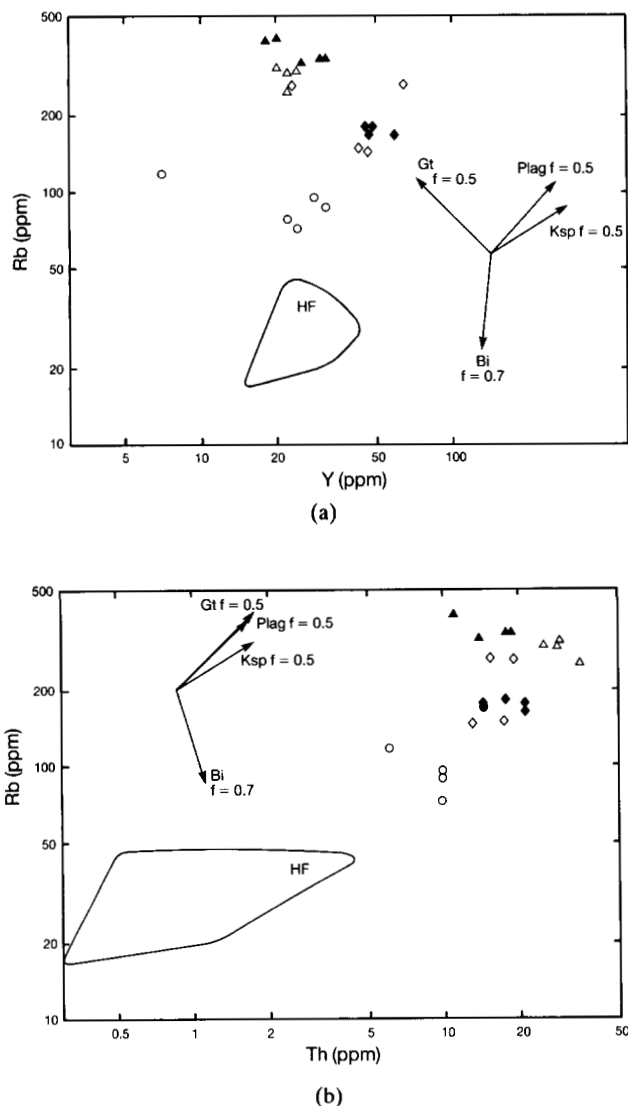


**Fig. 7.** Plots of Y and Th versus Rb for NE Palmer Land samples, symbols as in Fig. 2. Fractional crystallization vectors are after the Rayleigh law, for indicated  $f$  values. Distribution coefficients from Henderson (1982) except Th for alkali feldspar and Y for biotite and plagioclase (from Nash & Crecraft 1985).  $K_{\text{Th}}^{\text{garnet/liq}}$  and  $K_{\text{Y}}^{\text{alkali feldspar/liq}}$  arbitrarily set at 0;  $K_{\text{Th}}^{\text{garnet/liq}}$  estimated at 2. The field HF is for low Rb basalts of the Jurassic Hjort Formation, NE Palmer Land (Wever & Storey 1992).

contamination of subduction-related magmas rather than wholesale anatexis. Irrespective of this, magma genesis by crustal partial melting was clearly important during Triassic and Early Jurassic times along the proto-Pacific margin of Gondwana (Dalziel *et al.* 1987; Suárez *et al.* 1990; Storey *et al.* 1992) and this may have occurred during the initial stages of Gondwana fragmentation. The heat source responsible for the crustal melting was introduced by emplacement of mantle-derived mafic magmas formed by decompressional melting during extension. Their temporal and spatial association with subduction-related magmas and a more extensive within-plate Gondwana magmatic province suggests a possible causal relationship between subduction plate-margin processes, extension and the initial stages of Gondwana break-up (Storey *et al.* 1992).

## Conclusions

Geochemical and isotopic results indicate that Jurassic peraluminous granitic gneisses within the rear-arc region of NE Palmer Land formed by partial melting of pre-Mesozoic metasedimentary crust, mixed in various amounts with mafic magma which caused the anatexis. Crustal melting appears associated with the onset of formation of an ensialic back-arc basin, suggesting that extension within this part of the proto-Pacific margin of Gondwana may have commenced at around 200 Ma. The basalt magma was isotopically similar to approximately contemporaneous Karoo magmas associated with Gondwana break-up, although a genetic relationship between the Palmer Land and Karoo basalts is not certain. The generation of these peraluminous granites may be related to a zone of major crustal weakness which was reactivated during a period of Late Jurassic to Early Cretaceous arc and back-arc compression.

Fieldwork for this project was partly done in collaboration with P. D. Rowley and A. B. Ford, USGS, whose support we appreciate. Field work was made possible by field assistants P. Marquis and T. Simpson. We gratefully acknowledge T. Alabaster, and R. J. Pankhurst for useful discussions and constructive criticisms of earlier versions of this manuscript. The paper benefited from reviews by T. Alabaster, M. Atherton and S. Inger.

## References

- BREWSTER, T.S., HERGT, J.M., HAWKESWORTH, C.J., REX, D. & STOREY, B.C. 1992. Coats Land dolerites and the generation of Antarctic continental flood basalts. In: STOREY, B.C., ALABASTER, T. & PANKHURST, R.J. (eds) *Magmatism and the Causes of Continental Break-up*. Geological Society, London, Special Publications, **68**, 185–208.
- BRUHN, R.L., STERN, C.R. & DEWIT, M.J. 1978. Field and geochemical data bearing on the development of a Mesozoic volcano-tectonic rift zone and back-arc basin in southernmost South America. *Earth and Planetary Science Letters*, **41**, 32–46.
- DALZIEL, I.W.D., STOREY, B.C., GARRETT, S.W., GRUNOW, A.M., HERROD, L.D.B. & PANKHURST, R.J. 1987. Extensional tectonics and the fragmentation of Gondwanaland. In: COWARD, M.P., DEWEY, J.F. & HANCOCK, P.L. (eds) *Continental Extensional Tectonics*. Geological Society, London, Special Publications, **28**, 433–441.
- EWART, A. & HAWKESWORTH, C.J. 1987. The Pleistocene–Recent Tonga–Kermadec arc lavas: interpretation of new isotopic and rare earth element data in terms of a depleted mantle source model. *Journal of Petrology*, **28**, 495–530.
- FLOYD, P.A. 1985. Petrology and Geochemistry of oceanic intraplate sheet-flow basalts, Naru Basin, Deep Sea Drilling Project leg 89. In: MOBERLY, R., SCHLANGER, S.O. ET AL. (eds) *Initial Reports of the Deep Sea Drilling Project*, **89**, 471–497.
- GUST, D.A., BIDDLE, K.T., PHELPS, D.W. & ULIANA, M.A. 1985. Associated Middle to Late Jurassic Vulcanism and extension in southern South America. *Tectonophysics*, **116**, 223–253.
- HARRIS, C., MARSH, J.S., DUNCAN, A.R. & ERLANK, A.J. 1990. The petrogenesis of the Kirwan basalts of Dronning Maud Land, Antarctica. *Journal of Petrology*, **31**, 341–369.
- HARRIS, N.B.W. & INGER, S. 1992. Trace element modelling of pelite-derived granites. *Contributions to Mineralogy and Petrology*, **110**, 46–56.
- PEARCE, J.A. & TINDLE, A.G. 1986. Geochemical characteristics of collision-zone magmatism. In: COWARD, M.P. & RIES, A.C. (eds) *Collision Tectonics*. Geological Society, London, Special Publications, **19**, 67–81.
- HARRISON, S.W. & LOSKE, W.P. 1988. Early Palaeozoic U–Pb isotopic age for an orthogneiss from northwestern Palmer Land, Antarctic Peninsula. *British Antarctic Survey Bulletin*, **81**, 11–18.
- & PIERCY, B.A. 1990. The evolution of the Antarctic Peninsula magmatic arc: evidence from north-western Palmer Land. In: KAY, S.M. & RAPELA, C.W. (eds) *Plutonism from Antarctica to Alaska*. Geological Society of America Special Papers, **241**, 9–25.
- & — 1991. Basement gneisses in north-western Palmer Land: further evidence for pre-Mesozoic rocks in Lesser Antarctica. In: THOMSON, M.R.A., CRAME, J.A., THOMSON, J.W. (eds) *Geological Evolution of Antarctica*. Cambridge University Press, Cambridge, 341–344.
- HENDERSON, P. 1982. *Inorganic Geochemistry*. Pergamon, Oxford.
- HERGT, J.M., CHAPPELL, B.W., FAURE, G. & MESING, T.M. 1989. The geochemistry of Jurassic dolerites from Portal Peak, Antarctica. *Contributions to Mineralogy and Petrology*, **102**, 298–305.
- HILDRETH, W. & MOORBATH, S. 1988. Crustal contributions to arc magmatism in the Andes of central Chile. *Contributions to Mineralogy and Petrology*, **98**, 455–489.
- HOLE, M.J. 1986. *Time Controlled Geochemistry of Igneous Rocks of the Antarctic Peninsula*. PhD thesis, University of London.
- PANKHURST, R.J. & SAUNDERS, A.D. 1991. Geochemical evolution of the Antarctic Peninsula magmatic arc: the importance of mantle-crust interactions during granitoid genesis. In: THOMSON, M.R.A., CRAME, J.A., THOMSON, J.W. (eds) *Geological Evolution of Antarctica*. Cambridge University Press, Cambridge, 369–374.
- HUPPERT, H.E. & SPARKS, R.S.J. 1988. The generation of granitic magmas by intrusion of basalt into continental crust. *Journal of Petrology*, **29**, 599–624.
- INGER, S. & HARRIS, N. 1993. Geochemical constraints on leucogranite magmatism in the Langtang Valley, Nepal Himalaya. *Journal of Petrology*, **34**, 345–368.
- LEAT, P.T., STOREY, B.C. & PANKHURST, R.J. 1993. Geochemistry of Palaeozoic–Mesozoic Pacific rim orogenic magmatism, Thurston Island area, West Antarctica. *Antarctic Science*, **5**, 281–296.
- MCCULLOCH, M.T. & GAMBLE, J.A. 1991. Geochemical and geodynamical constraints on subduction zone magmatism. *Earth and Planetary Science Letters*, **102**, 358–374.
- MENEILLY, A.W., HARRISON, S.M., PIERCY, B.A. & STOREY, B.C. 1987. Structural evolution of the magmatic arc in northern Palmer Land, Antarctic Peninsula. In: MCKENZIE, G.D. (ed.) *Gondwana Six: Structure, Tectonics and Geophysics*. American Geophysical Union, Geophysical Monographs, **40**, 209–219.
- MILNE, A.J., & MILLAR, I.L. 1989. The significance of mid-Palaeozoic basement in Graham Land, Antarctic Peninsula. *Journal of the Geological Society, London*, **146**, 207–210.
- NASH, W.P. & CRECRAFT, H.R. 1985. Partition co-efficients for trace elements in silicic magmas. *Geochimica et Cosmochimica Acta*, **49**, 2309–2322.
- PANKHURST, R.J. 1982. Rb–Sr geochronology of Graham Land, Antarctica. *Journal of the Geological Society, London*, **139**, 701–711.
- 1983. Rb–Sr constraints on the ages of basement rocks of the Antarctic Peninsula. In: OLIVER, R.L., JAMES, P.R. & JAGO, J.B. (eds) *Antarctic Earth Science*. Australian Academy of Science, Canberra, 367–371.
- 1990. The Paleozoic and Andean Magmatic arcs of West Antarctica and southern South America. In: KAY, S.M. & RAPELA, C.W. (eds) *Plutonism from Antarctica to Alaska*. Geological Society of America Special Papers, **241**, 1–7.
- , HOLE, M.J. & BROOK, M. 1988. Isotope evidence for the origin of Andean granites. *Transactions of the Royal Society of Edinburgh*, **79**, 123–134.
- , MILLAR, I.L., GRUNOW, A.M. & STOREY, B.C. 1993. The pre-Cenozoic magmatic history of the Thurston Island crustal block, West Antarctica. *Journal of Geophysical Research*, **98**, 11835–11849.
- PARADA, M.A. 1990. Granitoid plutonism in central Chile and its geodynamic implications; A review. In: KAY, S.M. & RAPELA, C.W. (eds) *Plutonism from Antarctica to Alaska*. Geological Society of America Special Papers, **241**, 51–66.
- , RIJANO, S., SEPULVEDA, P., HERVE, M., HERVE, F., PUIG, A., MUNIZAGA, F., BROOK, M., PANKHURST, R.J. & SNELLING, N. 1988. Mesozoic and Cenozoic plutonic development in the Andes of central Chile (30°30′–32°30′S). *Journal of South American Earth Sciences*, **1**, 249–260.
- PEARCE, J.A., HARRIS, N.B.W. & TINDLE, A.G. 1984. Trace element discrimination diagrams for the tectonic interpretation of granitic rocks. *Journal of Petrology*, **25**, 956–983.
- POTTS, P.J. 1987. *A handbook of silicate rock analysis*. Blackie, Glasgow.
- RAPELA, C.W., PANKHURST, R.J. & HARRISON, S.M. 1992. Triassic ‘Gondwana’ granites of the Gastra district, North Patagonian Massif. *Transactions of the Royal Society of Edinburgh: Earth Sciences*, **83**, 291–304.
- RAPP, R.P., RYERSON, F.J. & MILLER, C.F. 1987. Experimental evidence bearing on the stability of monazite during crustal anatexis. *Geophysical Research Letters*, **14**, 307–310.
- SAUNDERS, A.D., TARNEY, J. & WEAVER, S.D. 1980. Transverse geochemical variations across the Antarctic Peninsula: implications for the genesis of calc-alkaline magmas. *Earth Planetary Science Letters*, **46**, 344–360.
- WEAVER, S.D. & TARNEY, J. 1982. The pattern of Antarctic Peninsula

- plutonism. In: CRADDOCK, C. (ed.) *Antarctic Geosciences*. University of Wisconsin Press, Madison, 305–314.
- SINGLETON, D.G. 1980. The geology of the central Black Coast, Palmer Land. *British Antarctic Survey Scientific Report*, **102**, 1–50.
- STAUDIGEL, H., ZINDLER, A., HART, S.R., LESLIE, T., CHEN, C.-Y. & CLAGUE, D. 1984. The isotope systematics of a juvenile intraplate volcano: Pb, Nd, and Sr isotope ratios of basalts from Loihi seamount, Hawaii. *Earth and Planetary Science Letters*, **69**, 13–29.
- STOREY, B.C. & ALABASTER, T. 1991. Tectono-magmatic controls on Gondwana break-up models: evidence from the proto-Pacific margin of Antarctica. *Tectonics*, **10**, 1274–1288.
- , —, HOLE, M.J., PANKHURST, R.J. & WEVER, H.E. 1992. Role of subduction-plate boundary forces during the initial stages of Gondwana break-up: evidence from the proto-Pacific margin of Antarctica. In: STOREY, B.C., ALABASTER, T. & PANKHURST, R.J. (eds) *Magmatism and the Causes of Continental Break-up*. Geological Society, London, Special Publications, **68**, 149–163.
- , WEVER, H.E., ROWLEY, P.D. & FORD, A.B. 1987a. The geology of the central Black Coast, eastern Palmer Land. *British Antarctic Survey Bulletin*, **77**, 145–155.
- , THOMSON, M.R.A. & MENEILLY, A.W. 1987b. The Gondwanian orogeny within the Antarctic Peninsula: a discussion. In: McKenzie, G.D. (ed.) *Gondwana Six: Structure, Tectonics, and Geophysics*. American Geophysical Union, Geophysical Monographs, **40**, 129–138.
- SUÁREZ, M. 1976. Plate tectonic model for southern Antarctic Peninsula and its relation to southern Andes. *Geology*, **4**, 211–214.
- , NARANJO, J.A. & PUIG, A. 1990. Mesozoic 'S-like' granites of the central and southern Andes; A review. In: KAY, S.M. & RAPELA, C.W. (eds) *Plutonism from Antarctica to Alaska*. Geological Society of America Special Papers, **241**, 27–32.
- SUN, S.-S. & McDONOUGH, W.F. 1989. Chemical and isotopic systematics of oceanic basalts: implications for mantle composition and processes. In: SAUNDERS, A.D. & NORRY, M.J. (eds) *Magmatism in the Ocean Basins*. Geological Society, London, Special Publications, **42**, 313–345.
- ULIANA, M.A., BIDDLE, K.T. & CERDAN, J. 1989. Mesozoic extension and the formation of Argentine sedimentary basins. *Bulletin of the American Association of Petroleum Geologists*, **46**, 599–614.
- VENNUM, W.R. & ROWLEY, P.D. 1986. Reconnaissance geochemistry of the Lassiter Coast Intrusive Suite, southern Antarctic Peninsula. *Geological Society of America Bulletin*, **97**, 1521–1533.
- WATT, G.R. & HARLEY, S.L. 1993. Accessory phase controls on the geochemistry of crustal melts and restites produced during water-undersaturated partial melting. *Contributions to Mineralogy and Petrology*, **114**, 550–566.
- WEVER, H.E. & STOREY, B.C. 1992. Bimodal magmatism in northeast Palmer Land, Antarctic Peninsula: geochemical evidence for a Jurassic ensialic back-arc basin. *Tectonophysics*, **205**, 239–260.
- , MILLAR, I.L. & PANKHURST, R.J. 1994. Geochronology and radiogenic isotope geology of Mesozoic rocks from eastern Palmer Land, Antarctic Peninsula: crustal anatexis in arc-related granitoid genesis. *Journal of South American Earth Sciences*, **7**, 69–83.
- WISE, D.U., DUNN, D.E. & ENGELDER, J.T. *ET AL.* 1984. *Fault-related rocks: Suggestions for terminology*. *Geology*, **12**, 391–394.

Received 24 November 1993; revised typescript accepted 10 March 1994.